Online Analysis of Remote Sensing Data for Agricultural Applications

Athanasios Karmas[*]
Institute for the Management
of Information Systems
"Athena" Research Center
Artemidos 6 & Epidavrou,
15125, Athens, Greece
karmas@imis.athena-
innovation.gr

Konstantinos Karantzalos
Remote Sensing Laboratory
National Technical University
of Athens
Zographou campus, 15780,
Athens, Greece
karank@central.ntua.gr

Spiros Athanasiou
Institute for the Management
of Information Systems
"Athena" Research Center
Artemidos 6 & Epidavrou,
15125, Athens, Greece
spathan@imis.athena-
innovation.gr

ABSTRACT

US Landsat and EU Sentinel missions -will shortly- provide massive multitemporal remote sensing data. Therefore, the development of efficient technologies for their direct manipulation and processing is of fundamental importance. Towards this direction, we present a WebGIS system for the online analysis of open remote sensing data and for precision agriculture applications. In particular, the core functionality consists of the Rasdaman Array Database Management System for storage, and the Open Geospatial Consortium Web Coverage Processing Service for data querying. Various queries have been designed and implemented in order to access and process multispectral satellite imagery. The WebGIS client, which is based on the OpenLayers and GeoExt javascript libraries, exploits these queries enabling the online ad-hoc spatial and spectral remote sensing data analysis. The currently under development framework is fully covering Greece with Landsat 8 multispectral data which are stored and pre-processed automatically in our hardware for demonstration purposes. The developed queries, which are focusing on agricultural applications, can efficiently estimate vegetation coverage, canopy and water stress over agricultural and forest areas. The online delivered remote sensing products have been evaluated and compared with similar processes performed from standard desktop remote sensing and GIS software.

Categories and Subject Descriptors

H.2.4 [**Systems**]: [Query processing, Heterogeneous Databases, Database Applications - Image databases]; I.4 [**Image Processing and Computer Vision**]: Computing Methodologies—*General - Image processing software*

---

[*]Corresponding author

General Terms

Algorithms, Management, Experimentation, Standardization, Verification

Keywords

Rasdaman, Precision Agriculture, Multitemporal, Multispectral, Satellite data, Geospatial data, WebGIS, WCPS

1. INTRODUCTION

There is a current need for intensive research, development and efficient technological solutions towards the exploitation of the increasing petabyte archives of geospatial (big) data. Along with the increasing volume and reliability of satellite, aerial, UAV and proximate earth observation sensors, the need for direct, high performance, big geospatial data processing and analysis systems, which are able to model and simulate a geo-spatially enabled content, is greater than ever.

The opening of the United States Geological Survey's Landsat data archive [20], the newly launched Landsat Data Continuity Mission [18], the EU Sentinel mission [15] as well as the EU open data policy [1] enabled the easy access to a record of historical data and related studies on monitoring mainly land cover/ land use changes, updating land national cover maps, detect the spatio-temporal dynamics, the evolution of land use change and landscape patterns.

With this increased data availability and the increasing open data policies, both in US and EU, research and development efforts should reflect the current demand on improving the capability to process directly big data and enable the efficient spatiotemporal modelling and monitoring. Therefore, the development of efficient technologies for the direct handling and processing on the server-side is of fundamental importance. In particular, current technological advances in the fields of computing power, computer resources and Internet speed has opened the way for online big geospatial data process and analysis enabling applications with significant scientific and industrial interest [12].

To this end, the developed *RemoteAgri* WebGIS system, is presented in this paper, which was designed towards the online analysis of open remote sensing data and precision agriculture applications. In particular, the core functionality consists of the Rasdaman Array Database Management

System (DBMS) for storage, and the Open Geospatial Consortium (OGC) Web Coverage Processing Service (WCPS) standard for data querying. Various WCPS queries have been designed and implemented in order to access and process multispectral satellite imagery. The WebGIS client is based on the OpenLayers and GeoExt javascript libraries. The currently under development framework is fully covering Greece with Landsat 8 multispectral data which are stored and pre-processed automatically in our hardware for demonstration purposes. The developed queries, which are focusing on agricultural applications, can efficiently estimate vegetation coverage, canopy and water stress over agricultural and forest areas.

2. RELATED WORK

Our WebGIS system (*RemoteAgri*), that has been designed and developed for the online analysis and visualization of open remote sensing data for agricultural applications, has been inspired mainly by PlanetServer [17] which is a service component of the EU-funded EarthServer project, aimed at serving and analyzing planetary data online.

EarthServer project[1] is creating an on-demand online open access and ad-hoc analytics infrastructure for massive (100+ TB) Earth Science data based on leading-edge Array Database platform and OGC WCPS standard. EarthServer establishes several, so-called, lighthouse applications, each of which poses distinct challenges on Earth Data analytics. These are Cryospheric Science, Airborne Science, Atmospheric Science, Geology, Oceanography and Planetary Science. In particular, for Planetary Science, PlanetServer application is being developed.

PlanetServer[2], is an online visualization and analysis service for planetary data that demonstrates how various technologies, tools and web standards can be used so as to provide big data analytics in an online environment. It is based on rasdaman [5],[6] Array DBMS as the data management platform and OGC WCPS standard [7] which allows submission of on-demand filtering and processing queries in a SQL-like query language meaning that it is a high-level, declarative query language resembling SQL for databases, but on multi-dimensional arrays. PlanetServer focuses on hyperspectral satellite imagery and topographic data visualization and analysis, mainly for mineralogical applications. Apart from the big data analytics part PlanetServer could aid in collaborative data analysis, as it is capable of sharing planetary data hosted on a database server and querying them from either any web client through any supported web browser or from any online processing service that adheres to OGC standard interfaces.

3. THE DEVELOPED WEB-GIS SYSTEM

The main objective of this work was to design and implement a framework for the online analysis of multispectral satellite imagery for agricultural applications. Various components and processing steps are involved in setting, running and utilizing the developed *RemoteAgri* WebGIS system.

The core functionality of our developed framework, consists of the Rasdaman Array DBMS for storage of remote sensing data and OGC WCPS interface standard for querying them. Rasdaman was selected as the core system of our implementation due to its proven robustness, novelty and efficiency in handling big geospatial data.

Currently, remote sensing data that are available in our database for processing by the *RemoteAgri* WebGIS system, are derived from the Landsat Data Continuity Mission (LDCM)[3]. The Landsat 8 OLI and TIRS instruments acquire multitemporal, multispectral data of fairly good spatial resolution. Landsat 8 raw data are downloaded, stored and pre-processed automatically through our system in a procedure that is described in subsection 3.1.

Vegetation detection, canopy estimation and water stress estimation are the key functionalities of the *RemoteAgri* system in its current version. These functionalities that come in the form of WCPS queries, utilize the Landsat 8 dataset and OGC WCPS interface standard in order to derive remote sensing information and produce respective color maps that hold this information.

The current *RemoteAgri* hardware is a 8-core machine with 32 GB RAM running Debian GNU/Linux (Release 7.5), Apache Tomcat 6 and the open source rasdaman community version 8.5. Under this demonstration environment, the stored and pre-processed remote sensing data are fully covering the Greek territory providing every apprx. 16 days satellite imagery from the beginning of the Landsat 8 mission (February 2013). The migration to a production environment is, already, scheduled.

The main components of the *RemoteAgri* Web-GIS system are presented in Figure 1 and are described thoroughly in the following sections.

3.1 Automated Data Acquisition, Storage and Preprocessing

As far as the download, storage and pre-processing stages of remote sensing data through our system are concerned, a number of Python scripts were developed which control, facilitate and automate the entire operation. Focusing on automation, firstly a script responsible for checking in the Landsat 8 archive for any newly acquired dataset, downloads any new one that will be found. Then another script archives the data *i.e.,* uncompresses them and performs all necessary image pre-processing radiometric correction steps that are required.

Regarding the radiometric correction steps, the USGS's (Unites States Geological Survey) instructions were followed in using the Landsat 8 product[4]. The standard Landsat 8 products provided by the USGS EROS Center consist of quantized and calibrated scaled Digital Numbers (DN) representing multispectral image data acquired by both the Operational Land Imager (OLI) and Thermal Infrared Sensor (TIRS). The products are delivered in 16-bit unsigned integer format and can be rescaled to the Top Of Atmosphere (TOA) reflectance and/or radiance using radiometric rescaling coefficients provided in the product metadata file (MTL file). The MTL file also contains the thermal constants needed to convert TIRS data to the at-satellite brightness temperature.

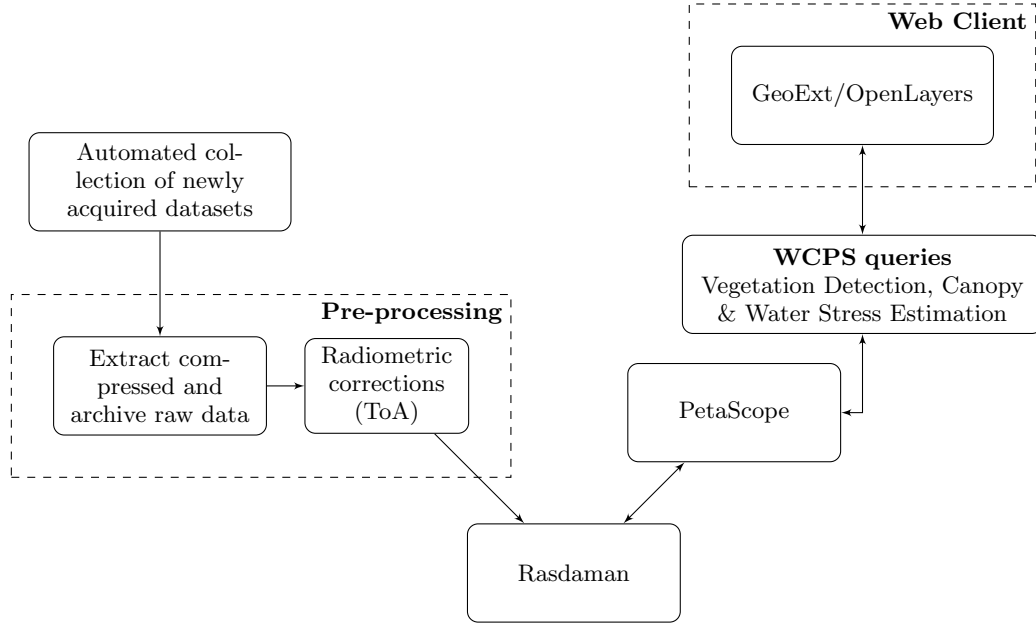For the conversion of OLI and TIRS band data to TOA

Figure 1: The components of the *RemoteAgri* WebGIS system.

spectral radiance the following equation was used:

$$Ll = Ml \cdot Qcal + Al \qquad (1)$$

where:
Ll = TOA spectral radiance (Watts/(m2 * srad * μm))
Ml = Band-specific multiplicative rescaling factor from the metadata.
$Qcal$ = Quantized and calibrated standard product pixel values (DN).
Al = Band-specific additive rescaling factor from the metadata.

For the conversion of DN values to TOA reflectance for OLI data the following equation was used:

$$rl' = Mr \cdot Qcal + Ar \qquad (2)$$

where:
rl' = TOA planetary reflectance, without correction for solar angle.
Mr = Band-specific multiplicative rescaling factor from the metadata.
Ar = Band-specific additive rescaling factor from the metadata.
$Qcal$ = Quantized and calibrated standard product pixel values (DN)

TOA reflectance with a correction for the sun angle is then:

$$rl = \frac{rl'}{sin(fse)} \qquad (3)$$

where:
rl = TOA planetary reflectance
fse = Local sun elevation angle. The scene center sun elevation angle in degrees is provided in the metadata.

For the conversion of spectral radiance from TIRS band data to brightness temperature the following equation was used:

$$T = \frac{K_2}{ln(\frac{K_1}{Ll} + 1)} \qquad (4)$$

where:
T = At-satellite brightness temperature (K).
Ll = TOA spectral radiance (Watts/(m2 * srad * μm)).
K_1 = Band-specific thermal conversion constant from the metadata.
K_2 = Band-specific thermal conversion constant from the metadata.

After the pre-processing stages, data are ready to be inserted into the rasdaman database. Thereupon, a final script reads the delivered metadata and inserts the datasets and their metadata into the rasdaman database.

3.2 The Rasdaman Array Database Management System

Multi-dimensional arrays of large size are not supported by traditional database management systems. As a consequence, these data are served through custom-made ad hoc servers which support arrays, but, on the other hand, lack database features such as query languages, query optimization and parallelization, and access-efficient storage architectures. Array DBMSs however, support multi-dimensional arrays with unlimited size of dimensions while offering all the classical databases advantages. Rasdaman's architecture is based on transparent array partitioning, called tiling.

The rasdaman database of our system currently contains multi-temporal imagery from the Landsat-8 satellite that covers the entire Greek territory (approximately 45 paths & rows) from the beginning of the mission. Prior to the ingestion of data in rasdaman a data type for the Landsat-8

data needed to be defined. The definition follows:

```
struct Landsat8Pixel {unsigned short  coastal, blue,
            green,  red, nir, swir1, swir2, cirrus,
            tirs1, tirs2;};
typedef marray <Landsat8Pixel,2> Landsat8Image;
```

This type definition first defines the "pixel type" by setting the amount of bands and the value type for each band. In the second line, a raster type is created using the keyword "marray" standing for "multi-dimensional array" which is specified as being 2D, with completely open bounds in all directions; thus the rasdaman server will allow for coverages at any coordinate and with a dynamically growing extent.

In Section 3.4 the way to derive information from Landsat-8 datasets will be described using WCPS. WCPS queries in general use a for-clause to define input data and a return-clause to define which information is returned and in what form:

```
for data in (collection)
return encode(data.band, "form")
```

In our case, band is replaced by one of the Landsat8 spectral bands as the collection is multiband and form is replaced with png as the WebGIS client handles image results of PNG type.

WCPS queries are submitted to the rasdaman database server through PetaScope component [2]. PetaScope is a java servlet package which implements OGC standard interfaces thus allowing on demand submission of queries that process multidimensional arrays. Moreover it adds geographic and temporal coordinate system support. The result of the process of the WCPS query is returned to the client from PetaScope in either textual or image form.

3.3   Web Client

The Web client of the *RemoteAgri* system is heavily based on OpenLayers and GeoExt javascript libraries. It utilizes them so as to place WCPS image results as layers inside a map. In order to achieve this metadata need to be determined. These metadata are the coordinates of the vertices of the bounding box that defines an Area Of Interest (AOI) that the user has specified and the name of the collection in the rasdaman database that hosts the image which contains the given AOI.

The coordinates of the bounding box that defines an AOI are recorded on completion of the definition of the AOI by the user. Then a server-side script utilizes them so as to find the collection that contains the AOI. The returned metadata are then processed in order to form the WCPS query that will be sent to PetaScope.

The coordinates that define the areal extent of the AOI are again used when the result image is retrieved from PetaScope to place the derived PNG image at its correct location in the WebGIS 's OpenLayers map. This allows for spectral data analysis in a WebGIS environment.

RemoteAgri system uses PetaScope and the image layer capability from OpenLayers to add results obtained from WCPS to the Openlayers map. The results can therefore be compared with overlapping visual imagery data from various sources. In Figure 2 a snapshot of the *RemoteAgri* system is displayed.

3.4   WCPS Queries

Once all necessary metadata have been determined the WCPS query that will process the Landsat 8 dataset is formed. In this subsection we present the WCPS queries that have been implemented and are related to certain agricultural applications.

3.4.1   Vegetation Detection

The detection of vegetation and its separation from the other terrain object and classes is the primary task. However, the spatial heterogeneity is an important property of natural landscapes that describes the variability of the observed surface properties in space. Simple vegetation detection methods which are based on vegetation indices, spectral band ratios, *etc.,* aren't separating the different vegetation types. The landscape of cropland mainly consists of a soil background and crops. The reflectivity characteristics of these two surface features differ completely in the red and NIR bands [10]. The soil spectrum varies over a wide range of length scales due to soil biogeochemical constituents (texture, organic matter content), moisture and surface roughness. A decrease in soil moisture causes an increase in the NIR reflectance of that soil. The relatively high radiation absorption capacity of chlorophyll in the red band leads to a decrease or saturation of the red reflectance of a canopy.

In a similar way with recent research efforts [13],[9] and since the queries do not allow algorithmic iterations during their parsing the NDVI (Normalized Difference Vegetation Index) was employed in order to detect the vegetation in a given region. In particular, the query performs vegetation detection based on the calculation of NDVI against a threshold value *vd*.

NDVI ranges between -1 and 1, with -1 meaning total absence of vegetation and 1 meaning dense presence of healthy vegetation. When NDVI is calculated against a threshold value we are able to discern vegetation, since for a certain threshold value all pixels that have NDVI value greater than the threshold indicate vegetation presence with a very high probability.

An example of a vegetation detection query follows:

```
// QUERY
// vegetation detection

for c in (L8_im_path_row) return encode
 (trim( (char)
  (((((c.nir - c.red)/(c.nir + c.red )) > vd )
  * 255),
  {x(22.62990426269617:22.76174020019607),
   y(40.54366380985645:40.70209989244132)}
  ), "png")
```

3.4.2   Canopy Estimation

Canopy estimation is a key task of fundamental importance for various agricultural applications. Therefore, given the importance of pigments to plant functioning, a greater effort has been concentrated to determine and quantify the relationship between gross primary production (GPP), and canopy chlorophyll (Chl) content which is the main photosynthetic pigment. Their proxy, the leaf area index (LAI)
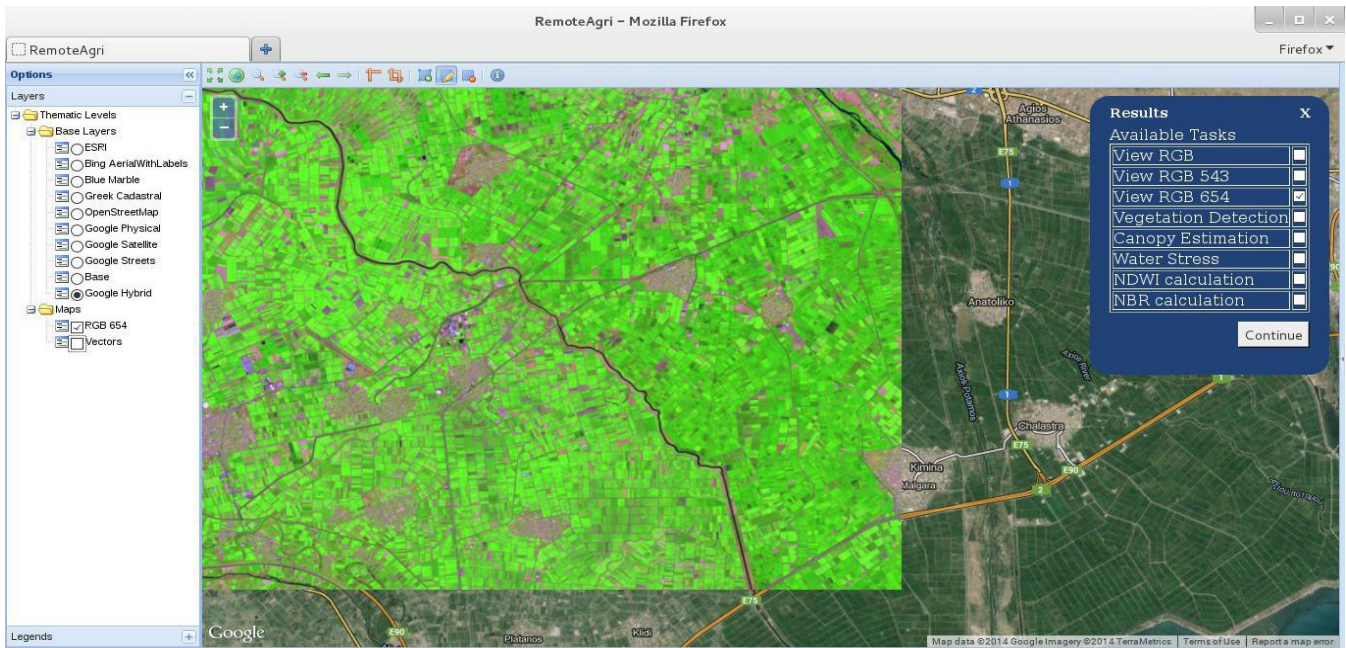
Figure 2: The *RemoteAgri* Web Client for the online analysis of remote sensing data for agricultural applications. In this particular snapshot, the *RemoteAgri* system has calculated a false color composite (RGB 654) over an area near Axios Delta in Greece and the result is depicted as an image layer overlay. Regions covered by any type of vegetation are shown with green color tones, since vegetation strongly reflects in the NIR band.

which is used as quantitative measures for canopy estimation and plant greenness is related with different vegetation indices with both broad and narrow bands.

In particular, Baret et al. [4] observed that canopy Chl content is a close proxy of canopy level N content and claimed that N status could be assessed through Chl content. Recent studies indicate, also, strong correlations between leaf chlorophyll (Chl) content and N content [8]. Close relationships were reported, moreover, between gross primary production, green LAI and canopy chlorophyll content [11].

Although, there isn't, still, a universal algorithm or regression model [16] that has been validated for all crops towards the efficient LAI estimation, in this study we employ the standard NDVI for all observed crops in the agricultural field. The Canopy Estimation query is based on the vegetation detection query and hence on the NDVI index.

For those areas that have been detected to contain vegetation a further classification is performed that indicate possible relations with crop vigor and LAI. For practical and visualisation purposes the output is determined by zoning the different canopy levels. The values of the NDVI which are greater than a certain threshold (*i.e., ce1, ce2, etc.*) are slitted into non overlapping intervals. Each interval is marked with a different color. Lighter colors indicate less vigorous crops. The output image of this query is an artificial color map that holds and pictures all the previously mentioned information.

The implemented WCPS query script follows:

```
// QUERY
// canopy estimation

for c in (L8_im_path_row) return encode
```

```
(trim(struct{
 red: (char)
 (((((c.nir - c.red)/(c.nir + c.red )) > ce1) *
  (((c.nir - c.red)/(c.nir + c.red )) <= ce2 )
   * 255) +
 (((((c.nir - c.red)/(c.nir + c.red )) > ce2) *
  (((c.nir - c.red)/(c.nir + c.red )) <= ce3 )
   * 255) +
 (((((c.nir - c.red)/(c.nir + c.red )) > ce3) *
  (((c.nir - c.red)/(c.nir + c.red )) <= ce4 )
   * 0) +
 (((((c.nir - c.red)/(c.nir + c.red )) > ce4) *
  (((c.nir - c.red)/(c.nir + c.red )) <= ce5 )
   * 0) +
 (((((c.nir - c.red)/(c.nir + c.red )) > ce5) *
  (((c.nir - c.red)/(c.nir + c.red )) <= ce6 )
   * 0) ;
 green: (char)
 ..similar..

 blue: (char)
 ..similar..

 }, {x(22.62990426269617:22.76174020019607),
 y(40.54366380985645:40.70209989244132)}),"png")
```

3.4.3 Water stress estimation

Along with the crop yield and gross primary production estimation through the canopy and leaf area index mapping, the crop stress estimation is the other key component for most agricultural applications. Optical remote sensing techniques has been studied a lot for the detection of stress
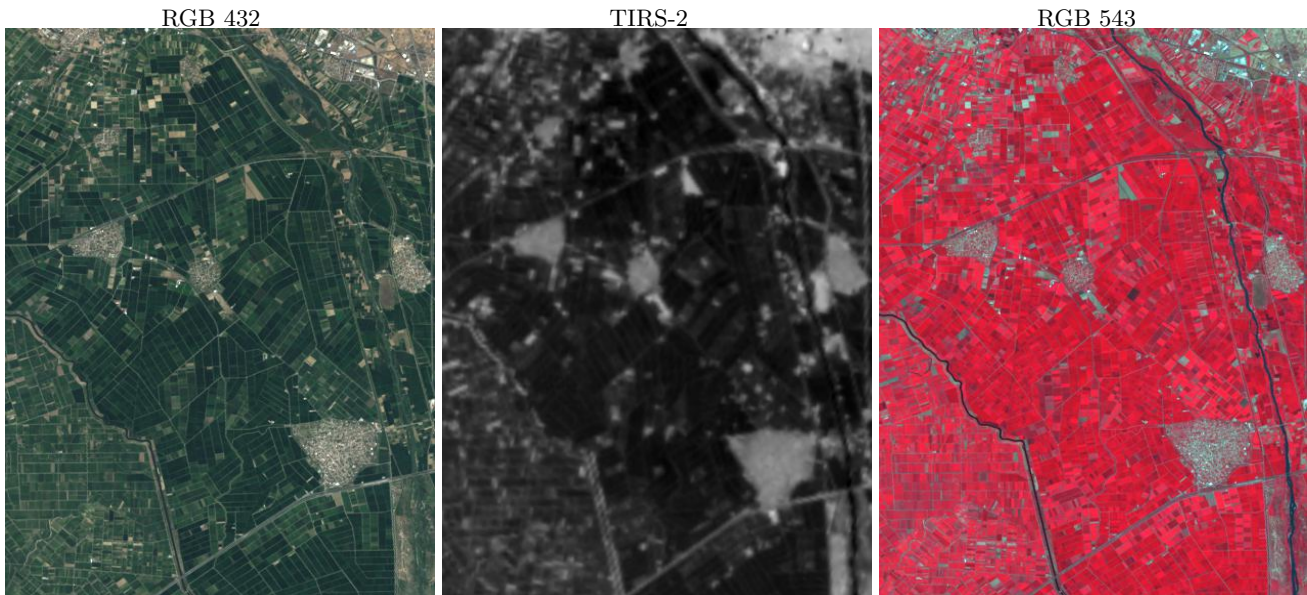
Figure 3: A case study from a Landsat-8 dataset near the Axios Delta, Greece acquired in July 2013. The natural (RGB 432) color composite is shown in the left part. The TIRS-2 thermal band is shown on the middle and a false color composite (RGB 543) is shown in the right part.

in vegetation. Various approaches have been developed to detect water stress from thermal infrared data, including the crop water stress index (CWSI). Several studies found that the standard deviation of canopy temperature can be used to quantify water deficit for low and moderately stressed crops [14].

Moreover, the accurate and cost-effective monitoring on water use, quantified at the scale of human influence, has been a long-standing critical need for a wide range of applications [3]. Apart from the irrigated water amount, quantifying, furthermore, evapotranspiration from irrigated crops is vital to management of water resources in areas of water scarcity, and detailed maps enable managers to more judiciously allocate available water among agricultural, urban, and environmental uses. The actual rate of water use by vegetation can deviate significantly from potential evapotranspiration rates (as regulated by atmospheric demand for water vapor) due to impacts of drought, disease, insects, vegetation amount and phenology, and soil texture, fertility and salinity.

Focusing on a simplified query structure, in order to detect the different water stress levels we employ the canopy temperature observations which can be used to quantify water deficit for low and moderately stressed crops. Concentrating again in the detected vegetation regions the information from the TIRS thermal sensor is employed. For practical and visualisation purposes after an initial min−max stretch on the raw intensity values, the intensity is zoned/mapped into 6-8 categories by splitting the values into non overlapping intervals (*i.e., ws1, ws2, etc.*) . The higher the values the higher the probability of water stress in irrigated croplands. In a similar way with the previous query, the result is an artificial color map which pictures information regarding the canopy temperature and the associated crop water stress. The implemented WCPS query follows:

```
// QUERY
```

```
// water stress estimation

for c in (L8_im_path_row) return encode
 (trim(struct{
  red: (char)
  (((((c.nir - c.red)/(c.nir + c.red )) > vg) *
   (((c.4 - min(c.4))/(max(c.4)-min(c.4))) < ws1)
   * 51) +
  (((((c.nir - c.red)/(c.nir + c.red )) > vg) *
   (((c.4 - min(c.4))/(max(c.4)-min(c.4))) >= ws1)
   *(((c.4 - min(c.4))/(max(c.4)-min(c.4))) < ws2)
    * 0) +
  (((((c.nir - c.red)/(c.nir + c.red )) > vg) *
   (((c.4 - min(c.4))/(max(c.4)-min(c.4))) >= ws2)
   *(((c.4 - min(c.4))/(max(c.4)-min(c.4))) < ws3)
   * 102) +
  (((((c.nir - c.red)/(c.nir + c.red )) > vg) *
   (((c.4 - min(c.4))/(max(c.4)-min(c.4))) >= ws3)
   *(((c.4 - min(c.4))/(max(c.4)-min(c.4))) < ws4)
    * 0) +
  (((((c.nir - c.red)/(c.nir + c.red )) > vg) *
   (((c.4 - min(c.4))/(max(c.4)-min(c.4))) >= ws4)
   *(((c.4 - min(c.4))/(max(c.4)-min(c.4))) < ws5)
   * 255) +
  (((((c.nir - c.red)/(c.nir + c.red )) > vg) *
   (((c.4 - min(c.4))/(max(c.4)-min(c.4))) >= ws5)
    * 255)

  green: (char)
  ..similar..

  blue: (char)
  ..similar..

 }, {x(22.62990426269617:22.76174020019607),
 y(40.54366380985645:40.70209989244132)}),"png")
```

Vegetation detection   Canopy estimation   Water stress estimation

<table>
<tr><td>🟥</td><td>0.5   – 0.52</td></tr>
<tr><td>🟨</td><td>0.52 – 0.55</td></tr>
<tr><td>🟩</td><td>0.55 – 0.575</td></tr>
<tr><td>🟩</td><td>0.575 – 0.6</td></tr>
<tr><td>🟩</td><td>> 0.6</td></tr>
</table>

□ vegetation

■ no vegetation

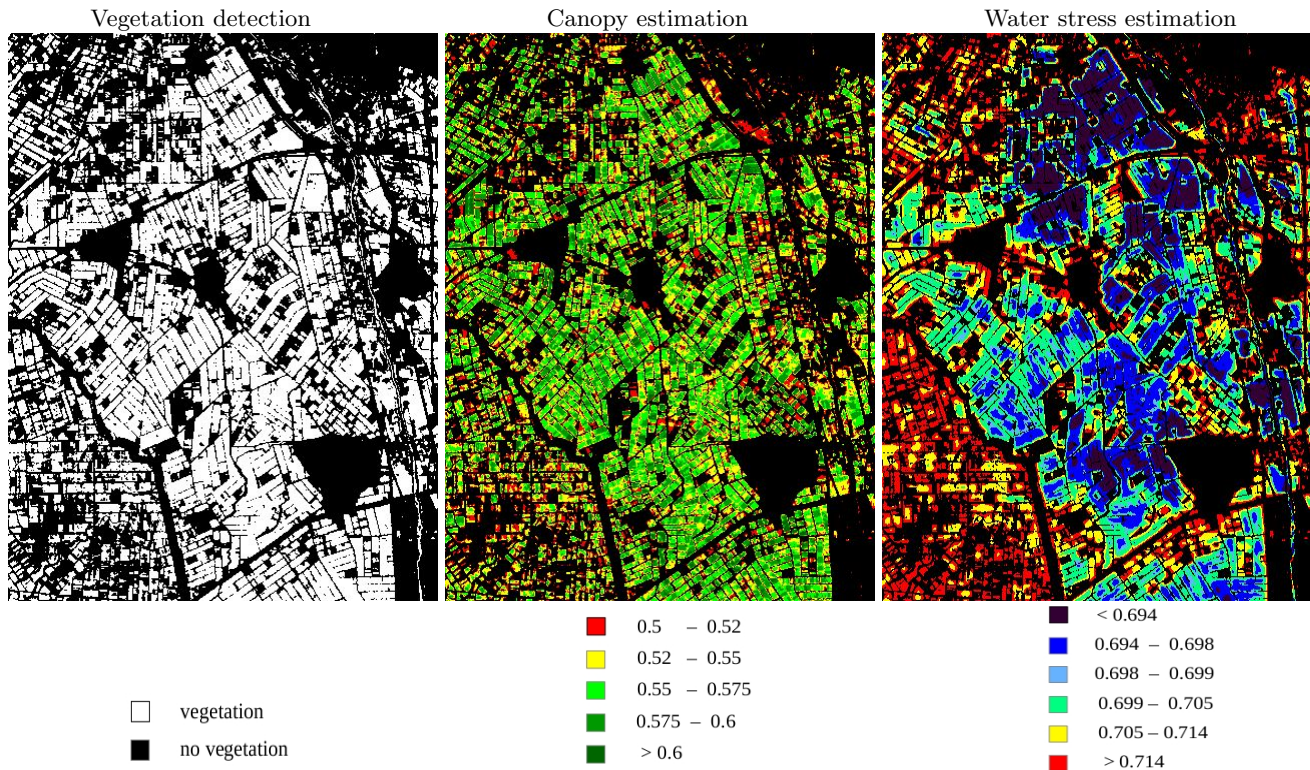|	
⬛	< 0.694
🟦	0.694 − 0.698
🟦	0.698 − 0.699
🟩	0.699 − 0.705
🟨	0.705 − 0.714
🟥	> 0.714

Figure 4: Experimental results from the _RemoteAgri_ server after the application of the "agricultural" queries on irrigated croplands near the Axios Delta, Greece. The detected vegetation is shown on the left part in a binary format. A map displaying the different levels (density) of crop canopy is shown on the middle, where red and yellow regions have been computed with lower densities and green areas with higher. A map displaying the different water stress levels associated with the canopy temperature is shown on the right part, where the yellow and red areas have been detected with higher water stress levels.

4. EXPERIMENTAL RESULTS AND EVALUATION

Several experiments were conducted in different Greek agricultural regions and at different seasons and dates. The goal was to tune the different parameters regarding the specific threshold for the vegetation detection and the zoning levels, intensity values intervals, when displaying the produced agricultural maps. However, there is, still, important work to be done towards the fully automation of the detection procedure since, yet, there isn't an established and fully validated operational pre-processing procedure for the Landsat-8 datasets. In particular, there are still a number of challenges that should be addressed [19] in order to exploit raw big remote sensing data and transform them to big geospatial reflectance surfaces. The most important one is automation during the main pre-processing procedures for the radiometric, atmospheric and geometric corrections/ calibration including i) geometric correction, ii) calibration of the satellite signal to obtain 'Top of the Atmosphere' radiance, iii) atmospheric correction to estimate surface reflectance, iv) topographic correction, and v) relative radiometric normalization between images obtained at different dates.

In the following Figure 3, Figure 4 and Figure 5 experimental results after the application of the main "agricultural" queries of the _RemoteAgri_ Web-GIS system are presented. In particular, results are shown from two Greek

agricultural areas with irrigated croplands. The first one is near the Axios Delta in the region of Central Macedonia. The summer rice crops are dominating the area (around 70%) while cotton and corn crops follow. This region was of specific interest due to the importance of a cost-effective crop canopy and stress estimation after the significant cotton yield loss during 2012. A second case study was near the Vegoritida Lake in the region of Epirus. The summer corn crops are dominating the area (around 80%) while other arable crops and vineyards follow. This region was of specific interest due to the importance effect of any agricultural practice in the surrounding NATURA 2000 ecosystem. It should be noted that during all our experiments all the parameters where left stable in order to directly compare the experimental results between the different region and between several acquisition dates and seasons.

In Figure 2, a snapshot of the _RemoteAgri_ web-client is shown. The main components of the web-client are demonstrated. On the left side a listing of the different base layers of the OpenLayers map can be found along with their Overlays which include the help vectors layers as well as the obtained image results from the WCPS. The GeoExt toolbar lays at the top. Among the different actions, a feature control is used for drawing a polygon on the OpenLayers map. This defines an Area Of Interest (AOI) for which the different WCPS queries are executed. Furthermore, all the base layers and overlays are displayed in the map panel. Last but not least, from the "Tasks" pop-up window the user can

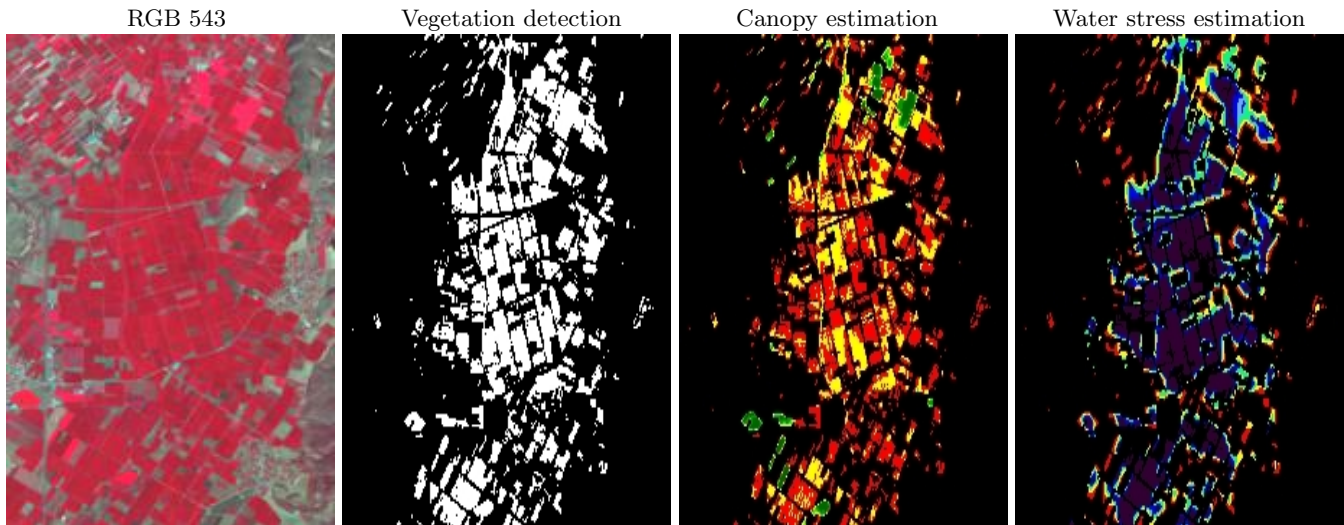| RGB 543 | Vegetation detection | Canopy estimation | Water stress estimation |

Figure 5: Experimental results from the *RemoteAgri* server after the application of the "agricultural" queries on irrigated croplands near Vegoritida Lake, Greece. The detected vegetation is shown on the left part in a binary format. A map displaying the different levels (density) of crop canopy is shown on the middle, where red and yellow regions have been computed with lower canopy densities. A map displaying the different water stress levels associated with the canopy temperature is shown on the right part, where the blue areas have been detected with low water stress levels.

select the type of the query/task that will be executed on the selected AOI.

In Figure 3, Landsat-8 data acquired in July 2013 are shown near the Axios Delta, Greece. The natural (RGB 432) color composite is shown in the left part of the figure. The TIRS-2 thermal band is shown on the middle and a false color composite (RGB 543) is shown in the right part of the figure. In Figure 4, experimental results after the application of the main "agricultural" queries on the irrigated croplands near the Axios Delta are presented. The detected vegetation is shown on the left part of the figure in a binary format. A map displaying the different levels (density) of crop canopy is shown on the middle of the figure, where red and yellow regions have been computed with lower densities and green areas with higher. A map displaying the different water stress levels associated with the canopy temperature is shown on the right part, where the yellow and red areas have been detected with higher water stress levels. These results have been validated with the same processes performed under a standard desktop GIS software (*QGIS*).

In Figure 5, experimental results after the application of the main "agricultural" queries of the *RemoteAgri* system are presented for the irrigated croplands near Vegoritida Lake, Greece. The detected vegetation is shown on the left part of the figure in a binary format. A map displaying the different levels (density) of crop canopy is shown on the middle, where red and yellow regions have been computed with lower canopy densities. A map displaying the different water stress levels associated with the canopy temperature is shown on the right part, where the blue areas have been detected with low water stress levels. The validation with a standard desktop GIS software (*QGIS*) and the inter-comparison between these two regions indicated that the canopy levels of the Axios Delta crops are higher than those near the Vegoritida Lake. However, the water stress levels in the Axios Delta crops are, also, higher than those in the Vegoritida region. This was, also, the case for the other acquisition dates up to

early October where the harvest period has begun for most of the crops.

5. CONCLUSIONS AND FUTURE PERSPECTIVES

In this paper, a WebGIS system capable of handling and analyzing online remote sensing data and for agricultural applications was presented. It was shown, at a demonstration level, that rasdaman as the back-end, WCPS standard and a webclient (utilizing the OpenLayers and GeoExt javascript libraries) as the front-end can be bind together. Based on this framework the developed *RemoteAgri* system is a robust and efficient WebGIS platform with the potential to evolve to a real-time agricultural monitoring system. Several excremental results from the online delivered remote sensing agricultural map/products have been evaluated, compared and validated based on similar processes from standard desktop remote sensing and GIS software.

Future work consists of bulk ingestion of geodata into the rasdaman database from various sensors and open data sources in order evaluate its performance on handling and processing online big geodata. The constant update and integration of the latest validated radiometric and atmospheric correction practices is on top of the list during the future development tasks regarding the queries and data pre-processing scripts. Furthermore, in addition to WCPS standard we plan to incorporate several other OGC standard interfaces in our system such as WPS (Web Processing Service), WCS (Web Coverage Service) and WMS (Web Map Service) so as to compensate for more intensive processing and analysis remote sensing algorithms in order to offer various Remote Sensing and GIS processing functionalities over the web. Further development of the webclient is on schedule as well as the development of an Android application so that our client can be viewed from any mobile device.

6. ACKNOWLEDGMENTS

7. REFERENCES

[1] COMMISSION DECISION of 12 december 2011 on the reuse of Commission documents (2011/833/eu). *Official Journal of the European Union*.

[2] A. Aiordachioaie and P. Baumann. Petascope: An open-source implementation of the ogc wcs geo service standards suite. In M. Gertz and B. Ludascher, editors, *Scientific and Statistical Database Management*, volume 6187 of *Lecture Notes in Computer Science*, pages 160–168. Springer Berlin Heidelberg, 2010.

[3] M. C. Anderson, R. G. Allen, A. Morse, and W. P. Kustas. Use of landsat thermal imagery in monitoring evapotranspiration and managing water resources. *Remote Sensing of Environment*, 122:50–65, 2012.

[4] F. Baret, V. Houles, and M. Guerif. Quantification of plant stress using remote sensing observations and crop models: The case of nitrogen management. *Journal of Experimental Botany*, 58(4):869•880, 2007.

[5] P. Baumann. Management of multidimensional discrete data. *The VLDB Journal*, 4(3):401–444, 1994.

[6] P. Baumann. Array databases and raster data management. In *In: T. Ozsu, L. Liu (eds.), Encyclopedia of Database Systems*. Springer, 2009.

[7] P. Baumann. The OGC web coverage processing service (WCPS) standard. *GeoInformatica*, 14(4):447–479, 2010.

[8] L. N. Deel, B. E. McNeil, P. G. Curtis, S. P. Serbin, A. Singh, K. N. Eshleman, and P. A. Townsend. Relationship of a landsat cumulative disturbance index to canopy nitrogen and forest structure. *Remote Sensing of Environment*, 118:40–49, 2012.

[9] Y. Ding, K. Zhao, X. Zheng, and T. Jiang. Temporal dynamics of spatial heterogeneity over cropland quantified by time-series ndvi, near infrared and red reflectance of landsat 8 OLI imagery. *International Journal of Applied Earth Observation and Geoinformation*, 30:139–145, 2014.

[10] A. Gitelson, Y. Kaufman, R. Stark, and D. Rundquist. Novel algorithms for remote estimation of vegetation fraction. *Remote Sensing of Environment*, 80:76–87, 2002.

[11] A. A. Gitelson, Y. Peng, T. J. Arkebauer, and J. Schepers. Relationships between gross primary production, green LAI, and canopy chlorophyll content in maize: Implications for remote sensing of primary production. *Remote Sensing of Environment*, 144:65–72, 2014.

[12] K. Kambatla, G. Kollias, V. Kumar, and A. Grama. Trends in big data analytics. *Journal of Parallel and Distributed Computing*, 2013.

[13] P. Li, L. Jiang, and Z. Feng. Cross-comparison of vegetation indices derived from landsat-7 enhanced thematic mapper plus (ETM+) and landsat-8 operational land imager (OLI) sensors. *Remote Sensing*, 6(1):310–329, 2013.

[14] E. Liu, aJiangui nd Pattey, J. R. Miller, H. McNairn, A. Smith, and B. Hu. Estimating crop stresses, aboveground dry biomass and yield of corn using multi-temporal optical data combined with a radiation use efficiency model. *Remote Sensing of Environment*, 114:1167–1177, 2010.

[15] S. Mecklenburg. GMES Sentinel Data Policy - An overview. In *GENESI-DR (Ground European Network for Earth Science Interoperations - Digital Repositories) workshop, ESAC, Villafranca, Spain*, 2009.

[16] A. L. Nguy-Robertson, Y. Peng, A. A. Gitelson, T. J. Arkebauer, A. Pimstein, I. Herrmann, A. Karnieli, D. C. Rundquist, and D. J. Bonfil. Estimating green LAI in four crops: Potential of determining optimal spectral bands for a universal algorithm. *Agricultural and Forest Meteorology*, 192•193:140–148, 2014.

[17] J. Oosthoek, J. Flahaut, A. Rossi, P. Baumann, D. Misev, P. Campalani, and V. Unnithan. Planetserver: Innovative approaches for the online analysis of hyperspectral satellite data from Mars. *Advances in Space Research*, pages 219–244, 2013.

[18] D. Roy, M. Wulder, T. Loveland, C. Woodcock, R. Allen, M. Anderson, D. Helder, J. Irons, D. Johnson, R. Kennedy, T. Scambos, C. Schaaf, J. Schott, Y. Sheng, E. Vermote, A. Belward, R. Bindschadler, W. Cohen, F. Gao, J. Hipple, P. Hostert, J. Huntington, C. Justice, A. Kilic, V. Kovalskyy, Z. Lee, L. Lymburner, J. Masek, J. McCorkel, Y. Shuai, R. Trezza, J. Vogelmann, R. Wynne, and Z. Zhu. Landsat-8: Science and product vision for terrestrial global change research. *Remote Sensing of Environment*, 145:154–172, 2014.

[19] G. Villa, J. Moreno, A. Calera, J. Amorss-Lspez, G. Camps-Valls, E. Domenech, J. Garrido, J. Gonzalez-Matesanz, L. Gsmez-Chova, J. A. Martnnez, S. Molina, J. J. Peces, N. Plaza, A. Porcuna, J. A. Tejeiro, and N. Valcarcel. Spectro-temporal reflectance surfaces: a new conceptual framework for the integration of remote-sensing data from multiple different sensors. *International Journal of Remote Sensing*, 34(9-10):3699–3715, 2013.

[20] M. A. Wulder, J. G. Masek, W. B. Cohen, T. R. Loveland, and C. E. Woodcock. Opening the archive: How free data has enabled the science and monitoring promise of landsat. *Remote Sensing of Environment*, 122:2–10, 2012.